Trend and abrupt changes in long-term geomagnetic indices

Hua Lu,[1] Yun Li,[2] Mark A. Clilverd,[1] and Martin J. Jarvis[1]

Received 29 November 2011; revised 8 March 2012; accepted 28 March 2012; published 17 May 2012.

[1] Advanced statistical methods are employed to analyze three long-term time series of geomagnetic activity indices (*aa*, IHV, and IDV) together with sunspot number (*Rz*) to examine whether or not the *aa* index can realistically represent long-term variations of geomagnetic activity. We make use of a decomposition method called STL, which is a time domain filtering procedure that decomposes a time series into trend, cyclic, and residual components using nonparametric regression. A Bayesian change point analysis is also applied to the geomagnetic indices, as well as to sunspot number, to detect abrupt changes that may be caused by either instrumental changes, calibration errors, or sudden changes in solar activity. Our analysis shows that all three long-term geomagnetic indices share a similar centennial-scale variation that resembles the long-term trend of sunspot number *Rz*. The amplitude ratio between the centennial-scale variation and 11-year cycle of *aa* and IHV are closely comparable. Overall, our analysis suggests that the majority of the changes in the *aa* index are controlled by solar activity. Instrumental change or site relocation has only a limited effect on the long-term trend of *aa*. This is in good agreement with those previous studies which have shown *aa* to be a reliable long-term index.

Citation: Lu, H., Y. Li, M. A. Clilverd, and M. J. Jarvis (2012), Trend and abrupt changes in long-term geomagnetic indices, *J. Geophys. Res.*, *117*, A05318, doi:10.1029/2011JA017422.

1. Introduction

[2] The *aa* index [*Mayaud*, 1972] has been commonly used to study the long-term change of solar-terrestrial phenomena and past variation in the near-Earth heliosphere. It is the longest continuous data series of an index that measures global geomagnetic activity. The *aa* index was initially designed to characterize the reaction of the Earth's upper atmosphere (e.g., magnetosphere and ionosphere) and magnetic field to the incoming solar wind. It is derived from a weighted average of the 3-hourly *K* indices from two near-antipodal, midlatitude observatories, one in Britain and one in Australia. At a given observatory, the *K* index, which is a ranked, dimensionless integer in the range of 0–9, indicates the maximum fluctuations of the horizontal component of the geomagnetic field measured at Earth's surface by a magnetometer during a 3-h interval. A site-dependent calibration is applied so that the occurrences of individual levels of *K* are about the same at all observatories [*Mayaud*, 1972]. The antipodal observatories used for measuring the *K*-indices have moved location twice in each hemisphere. The sites were initially at Greenwich (51°28′N, 0°0W) during the period of 1868–1925 and Melbourne (37°49′S, 144°58′E) during the period of 1868–1919. In the northern hemisphere, the observatory was first moved to Abinger (51°11′N 0°23′W, 1926–1956) and later to Hartland (50°59′N, 355°31′E, 1957–present). In Australia, Toolangi (37°32′S, 145°28′E, 1920–1979) and Canberra (35°17′S, 149°13′E, 1980–present) were used to continue the measurement. At each observatory change, a site correction was made for changes in geomagnetic latitude and local induction effects. This was achieved by running the two sites in parallel for 1 to 2 years, so that a calibration factor could be established to equalize the annual means of the old and new stations. For changes in the southern observatory, the normalization was carried out with respect to the normalized northern series.

[3] Several studies have shown a general increase of the *aa* index during the 20th century, most likely caused by long-term variations of solar activity [*Feynman and Crooker*, 1978; *Clilverd et al.*, 1998; *Cliver et al.*, 1998; *Lockwood et al.*, 1999; *Stamper et al.*, 1999]. However, other studies have questioned the validity of the long-term trend in the *aa* index because of the inhomogeneity induced by stations or instrumental changes and by site-specific normalization [*Svalgaard et al.*, 2003, 2004; *Svalgaard and Cliver*, 2005; *Mursula and Martini*, 2007]. For instance, the centennial increase of geomagnetic activity extracted from the *aa* index has been attributed to possible station inter-calibration in 1957 when the northern *aa* station was relocated from Abinger to Hartland [*Svalgaard et al.*, 2004], or to an instrumental change which occurred in 1938 at Abinger [*Svalgaard et al.*, 2003]. Those studies, based on alternative indices, have suggested a substantially reduced or close to zero long-term

[1]British Antarctic Survey, Cambridge, UK.
[2]CSIRO Mathematics, Informatics and Statistics, Wembley, Western Australia, Australia.

Corresponding author: H. Lu, British Antarctic Survey, High Cross, Madingley Road, Cambridge CB3 0ET, UK. (hlu@bas.ac.uk)

0148-0227/12/2011JA017422

trend in geomagnetic activity [*Svalgaard et al.*, 2004; *Svalgaard and Cliver*, 2005; *Mursula and Martini*, 2007].

[4] Conversely, other studies concluded that site relocation or instrumental changes cannot significantly affect the centennial-scale increase of the *aa* during the 20th century [*Clilverd et al.*, 2002, 2005; *Lukianova et al.*, 2009]. *Clilverd et al.* [2002] showed that instrumental changes might have caused ~2 nT artificial increase in total in the *aa* index, but such contamination is too small to cause the substantial increase of storm activity since the early 20th century. *Clilverd et al.* [2005] generated *aa* indices from *K*-indices taken from two alternative northern observatories, one in Finland that extends back to 1914 and another in Germany that extends back as 1890. These alternative *aa* series showed very similar trends to that in the official *aa*. *Lockwood et al.* [2009] suggested that the step-like change in the *aa* index in 1957 is only ~2 nT, which is considerably smaller than its centennial increase (~15 nT). *Lockwood et al.* [2009] also found that the alternative geomagnetic index IHV [*Svalgaard et al.*, 2004] in fact gave a long-term variation comparable with that deduced from *aa*. *Lukianova et al.* [2009] confirmed that the changes in the *aa* index associated with all four station re-locations were small compared with its centennial-scale increase. *Lockwood and Owens* [2011] show that *aa* and the new alternative geomagnetic index IDV give almost identical long-term variations in open solar flux and near-Earth interplanetary magnetic field (IMF).

[5] Because of the important role that the *aa* index has played in the past in terms of understanding the long-term behavior of Sun-Earth connections, it is crucial that we are able to differentiate the physically meaningful changes that are associated with long-term drift of solar wind characteristics from the artificial contamination introduced by observatory relocation, instrumental configuration and/or site-dependent calibration. As a step toward improved understanding of the centennial-scale variation of geomagnetic activity, here we employ advanced statistical methods to analyze three long-term time series of geomagnetic activity indices together with the sunspot number. Our main objectives are (1) to examine whether or not the *aa* index can realistically represent long-term variations of geomagnetic activity in comparison to other geomagnetic indices and (2) to examine and quantify the abrupt changes in the *aa* index that may be caused by either instrumental changes, calibration errors, or sudden changes in solar activity. To achieve the first goal, we decompose the three geomagnetic indices and the sunspot number into cyclic, trend and residual components using a time series decomposition method called Seasonal-Trend based LOESS [*Cleveland et al.*, 1990], which allows us to examine the differences among the long-term trends derived from the three geomagnetic indices and to compare them with the trend estimated from the sunspot number. For the second goal, we use a Bayesian analysis to detect abrupt changes in the occurrence of $K = 0$ in 3-hourly *K*-indices for the northern and the southern stations, and also in the ratio between these two time series which allows us to identify abrupt changes caused by site or instrumental changes. A similar analysis is also made to examine whether the abrupt changes in geomagnetic indices are linked to similar changes in the sunspot number. Together, these analyses allow us to quantify how much site-relocation, instrumental or calibration changes have played a role in contaminating the long-term trend in the official *aa* index.

2. Data

[6] Earth's magnetic field disturbances are the result of solar wind – magnetosphere coupling. Geomagnetic activity indices were conventionally designed to characterize magnetospheric disturbances due to magnetospheric substorms and magnetic storms. The widely used *aa* and *Ap* indices rank the geomagnetic field disturbances every 3 h. The strength of geomagnetic activity is largely determined by the southward component of the IMF to which the coupling between the interplanetary magnetic field (IMF) and the Earth's magnetosphere is most sensitive [*Newell et al.*, 2007]. To study long-term variations of geomagnetic activity, the annual averages of the *aa* index, covering 143 years (1968–2010), are used here. Annual mean planetary *Ap* index for the period of 1932–2010 is also used for comparison. In the annual averages, the indices were found to depend mainly on a combined effect of the IMF field strength *B* and solar wind speed *V* [*Lockwood and Owens*, 2011].

[7] To examine how much of any abrupt changes in *aa* might be linked to site or instrumental changes, the annual number of occurrences of $K = 0$ (K_0 hereafter), and other subgroups of *K* values for the same period, are estimated from 3-hourly *K*-indices from northern and southern *aa* stations.

[8] *Svalgaard et al.* [2004] developed an alternative long-term geomagnetic index called the inter-hourly variability (IHV) index, which was based on the inter-hourly variability of magnetograms at any single station around local midnight; it was defined as the sum of unsigned differences of hourly means for each geomagnetic component from one hour to the next over the 6-h interval around local midnight, where the solar daily variation is absent or minimal. The annual global composite IHV index was derived from individual IHV indices generated from 70 observatories equatorward of 55°, grouped in longitudinal sectors, as a mean over each calendar year. In this study, annual mean IHV index for the extended period of 1844–2010 is downloaded from http://www.leif.org/research/ and used to compare with the *aa* index.

[9] The third long-term geomagnetic index used here is the annual mean Inter-Diurnal Variability (IDV) index, which was introduced by *Svalgaard and Cliver* [2005]. The daily IDV index was estimated for a given geomagnetic observatory as the unsigned difference of the averaged horizontal component for the first hour after local midnight and the value from one hour after midnight between two consecutive days. The daily values were then averaged over a year and over all midlatitude stations so that site-specific and seasonal effects are minimized. The characterization of the IDV index is very similar to the *u*-measure of *Bartels* [1932]. More recently, *Svalgaard and Cliver* [2010] included more data (i.e., 143 versus 34 stations used by *Svalgaard and Cliver* [2005]) and extended IDV to include the earlier period of 1890–1909 and the time series was recently extended back to 1835 (L. Svalgaard, personal communication, 2011). In this study, annual mean IDV covering the period of 1835–2010 is used.

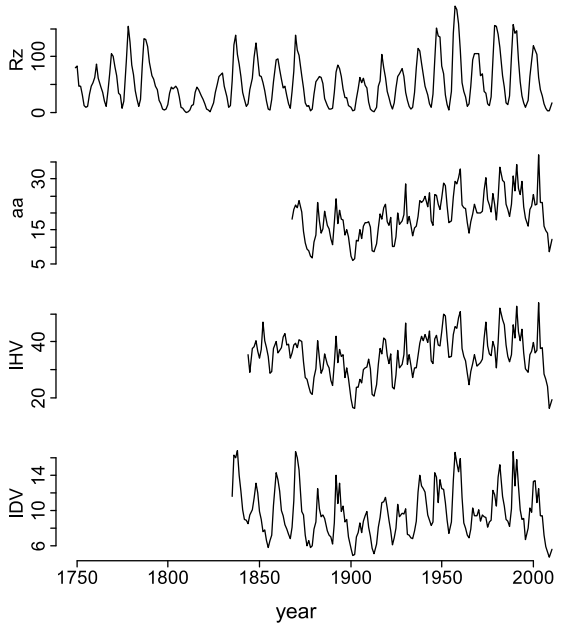

Figure 1. Time series of annual mean *Rz* (1749–2010), *aa* (1868–2010), IHV (1844–2010), and IDV (1835–2010).

[10] By using local nighttime hourly measurements, the IHV and IDV indices avoid the need to separate disturbances and quiet time variations and therefore avoid the need of ranking the disturbances. As a consequence, they are less subject to calibration errors as they do not require any station-based calibration as the *aa* and *A*p indices require. They also avoid extreme ultraviolet (EUV) induced regular variation. However, by relying on mid-night observations only, neither IHV nor IDV are able to provide temporal structure of storm or substorm variations that geomagnetic indices mainly aimed to measure. As such, IHV and IDV indices characterizing the variability of geomagnetic activity should be regarded as indicators of *long-term* changes in geomagnetic activity rather than direct measures of geomagnetic activity analogous to the *aa* and *Ap* indices.

[11] It is also worth noting that whereas *aa* is homogenous in its construction over the period of 1868–present, IHV and IDV do degrade in time pre-20th century, in which larger uncertainty was associated with annual IHV and IDV due to few stations being available during the time.

[12] The sunspot number (*Rz*) is compared with the trend and abrupt changes identified in the three geomagnetic indices. As well as being a proxy for studying the long-term change of solar activity at centennial time scales, *Rz* is also a proxy for solar electromagnetic radiation which creates and maintains the earth's ionosphere and the tidal winds in the atmosphere. Annual mean international sunspot number obtained from NOAA's National Geophysical Data Center (NGDC) (http://www.ngdc.noaa.gov/) from 1749 to 2010 is used here. Figure 1 compares the time series of the annual mean *Rz*, *aa*, IHV, and IDV.

3. Analysis Methods

[13] In order to compare the long-term trends of the geomagnetic indices with that from sunspot number, it is necessary to objectively exclude the effects due to the quasi-11-yr cyclic variation and irregular changes in the four time series under consideration, i.e., *Rz*, *aa*, IHV, and IDV. For this purpose, a decomposition method called STL that decomposes a time series into trend, cyclic component and residual components, through a sequence of locally weighted regression smoothing called LOESS [*Cleveland and Devlin*, 1988]. STL is a time domain filtering procedure that decomposes a time series with a known quasiperiodicity (quasi-11-yr in this case) using nonparametric regression. In a nutshell, STL decomposes a time series into three additive frequency components of variations: cyclic, trend and residual and supports robust statistical estimation of seasonal and trend components to limit the effect of outliers or other forms of aberrant data. Through the decomposition, it facilitates clearer assessment of the temporal behavior and relative scaling of each additive component. STL has, for example, been applied to separate woody and herbaceous vegetation cover using satellite data [*Lu et al.*, 2003], to forecast a soil dryness index [*Li et al.*, 2003], and to study long-term trends of synoptic-scale breaking Rossby waves in the Northern Hemisphere [*Isotta et al.*, 2008]. It is used here for the first time to study solar-geomagnetic connections. A detailed description of the decomposition procedure can be found in *Cleveland et al.* [1990] and it is briefly described in Appendix A.

[14] A Bayesian change point detection algorithm [*Barry and Hartigan*, 1993] has been applied to time series in economics [*Koop and Potter*, 1997], medicine [*Erdman and Emerson*, 2008; *Hegarty and Barry*, 2008], and biology [*Johnson et al.*, 2003] to identify abrupt changes. Here we use it to study sudden changes in geomagnetic indices and to analyze how those changes may be linked to either solar-induced changes, instrumental errors or site calibration. For this purpose, the 'bcp' package [*Erdman and Emerson*, 2007] is applied to the solar and geomagnetic activity time series. A brief description of the method is given in Appendix B. For simplicity and to facilitate presentation of the key results, we used probability $p = 0.8$ (or 80%) to discuss and compare the most likely change-point in a given time series under consideration. A detailed description of the implementation procedure can be found in *Erdman and Emerson* [2007] and it is briefly described in Appendix B.

4. Results

4.1. Century-Scale Variation of Geomagnetic Activity

[15] Figure 2 shows the cyclic, trend and residual components of sunspot number *Rz*, and the *aa*, IHV and IDV indices. It is clear that both the amplitude and periodicity of the 11-yr cyclic variation of *Rz* have undergone a centennial-scale variation that is closely linked to its trend component. Its amplitude is small when the trend troughs and large when the trend peaks. The magnitude of the centennial-scale variation in the trend of *Rz* is ~33.7 while the amplitude of its cyclic component is ~87.2. Thus, on average, the amplitude of centennial variation of *Rz* is ~39% of that of the Schwabe (11-yr) solar cycle.

[16] The trend of the *aa* index shows a centennial variation that resembles that of *Rz*. The amplitude of the 11-yr cyclic variation of *aa* also varies with its trend, but being larger at the trough and smaller at the peak; such behavior is opposite

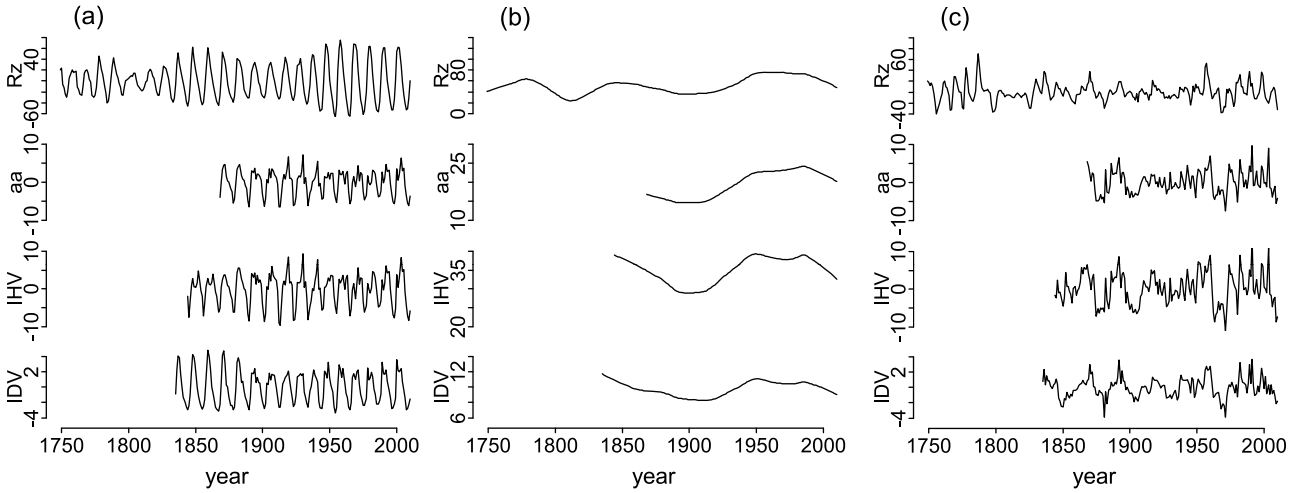

Figure 2. (a) Cyclic, (b) trend, and (c) residual components of annual mean *Rz*, *aa*, IHV and IDV (from top to bottom). For the ease of amplitude comparison, the lengths of vertical scales are set the same for each index.

to that of *Rz*. The amplitude of the centennial-scale variation of *aa* is ∼9.7 nT while the amplitude of its cyclic component is ∼11.9 nT. Thus, the amplitude of the centennial variation of *aa* is approximately 81% of its decadal variation.

[17] The centennial-scale variations in both IHV and IDV also resemble that of *Rz*. The relative magnitudes of trend versus cyclic component of the IHV index are ∼10.3 nT versus ∼12.9 nT, which gives a trend-cyclic ratio of 80%. For the IDV index, the amplitude of the trend is estimated as ∼2.8 nT compared to ∼5.9 nT of its cyclic component, which gives a trend-cycle ratio of 48%.

[18] In addition, the cyclic variations in *aa* and IHV have shown a double peak structure since solar cycle 13. The second peak, which occurs mostly in the declining phase of the solar cycle, tends to be stronger than the first peak, particularly during solar cycle 14–16 and the recent four solar cycles from 20 to 23. It has been suggested that the second peak in *aa* over an 11-yr solar cycle is induced by fast solar wind from the co-rotating interaction regions (CIRs) of solar corona holes, while the first peak that coincides mostly with the sunspot maximum is related to coronal mass ejections (CMEs) [*Gonzalez et al.*, 1999]. Figure 2b implies that the occurrence and/or the intensity of CMEs or CIRs were not uniformly distributed over the centennial-scale. Stronger, and/or more frequent than average, recurrent fast solar wind occurred during the periods of 1920–1940 and 1970–2000 than during other time periods.

[19] The quasi-11-yr cyclic variation in the IDV index differs from that in *aa* and IHV. There is also an apparent double peak structure in the IDV's 11-yr cyclic component but this double peak structure emerges mostly around solar maxima. Similar to *Rz*, the amplitude of the cyclic component of IDV varies with its centennial-scale trend, smaller at the trough and larger at the peak. The correlation coefficients among the four time series and their associated quasi-11-yr cyclic variation, centennial trend and residual components are given Table 1 for the period of 1868–2010 where all four time series overlapped. For the raw data, the highest correlation is between *aa* and IHV (0.96) and the second highest correlation is between *Rz* and IDV (0.85). For the decomposed components, the highest correlation is among the trends (all $r > 0.9$). The *aa* and IHV indices share almost identical cyclic components with $r = 0.99$ while the cyclic component of IDV best follows that of *Rz* ($r = 0.88$).

[20] Figure 3 shows the normalized centennial-scale trends in *Rz*, *aa*, IHV and IDV. The general shape and amplitude of the trends are in good agreement, suggesting all three geomagnetic indices share a similar centennial-scale variation and are controlled by long-term variations of solar activity. Nevertheless, the trend of *aa* differs subtly from those of IHV and IDV in two places. First, there was clear disagreement before 1860. This may be caused by data quality in the constructed IHV and IDV before 1872 [*Svalgaard and Cliver*, 2010] and to a smaller extent, due to the edge effect in STL decomposition. Second, the *aa* trend peaks at a different time than the trends of IHV and IDV. While IHV and IDV trends have double peaks, a larger peak in 1950 and a

Table 1. Correlation Coefficient Between *Rz* and Each of *aa*, IHV, and IDV at Different Component Levels Over 143 Years From 1868 to 2010 When Data for All These Time Series Are Available

Level	Variable	Rz	*aa*	IHV	IDV	Mean Amplitude
Raw data	*Rz*	1	0.59	0.57	0.85	-
	aa	0.59	1.00	0.96	0.79	-
	IHV	0.57	0.96	1.00	0.80	-
	IDV	0.85	0.79	0.80	1	-
Cycle	*Rz*	1	0.55	0.49	0.88	87.21
	aa	0.55	1.00	0.99	0.81	11.89
	IHV	0.49	0.99	1.00	0.76	12.91
	IDV	0.88	0.81	0.76	1	5.90
Trend	*Rz*	1	0.96	0.97	0.97	33.72
	aa	0.96	1.00	0.94	0.92	9.66
	IHV	0.97	0.94	1.00	0.98	10.29
	IDV	0.97	0.92	0.98	1	2.84
Residual	*Rz*	1	0.47	0.50	0.77	-
	aa	0.47	1.00	0.97	0.78	-
	IHV	0.50	0.97	1.00	0.80	-
	IDV	0.77	0.78	0.80	1	-

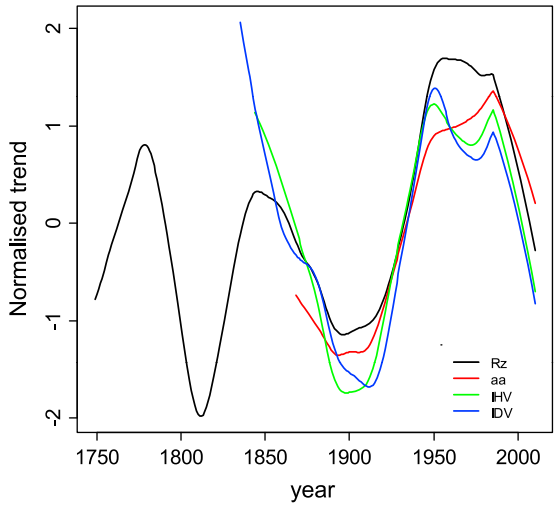

Figure 3. Normalized trend component of annual mean *Rz* (black), *aa* (red), IHV (green), and IDV (blue).

smaller one in 1985, the double peak structure is not clear in the *aa* trend and 1985 becomes the dominant peak.

4.2. Abrupt Changes in K Index and Their Origin

[21] It has been suggested that site relocation or instrumental changes might have caused an artificial increase of the long-term trend of *aa* [e.g., *Svalgaard et al.*, 2003, 2004]. In this section, we apply a Bayesian analysis to study abrupt changes in the annual occurrence of the *K* index for a given *K* value or a group of *K* values, and examine whether or not the detected changes can be linked to either solar, instrumental or site related changes. From these results and previous studies, we address the question: whether or not site-relocation and/or instrumental change induced a significant change in the long term trend of *aa*?

4.2.1. Changes That Are Linked to Solar Activity

[22] Figure 4 shows the annual occurrence of $K = 0$ for the northern ($K_{0,N}$, Figure 4 (left)) and southern ($K_{0,S}$, Figure 4 (right)) hemispheres and the abrupt change years (with a probability $p > 0.8$) detected by the Bayesian analysis

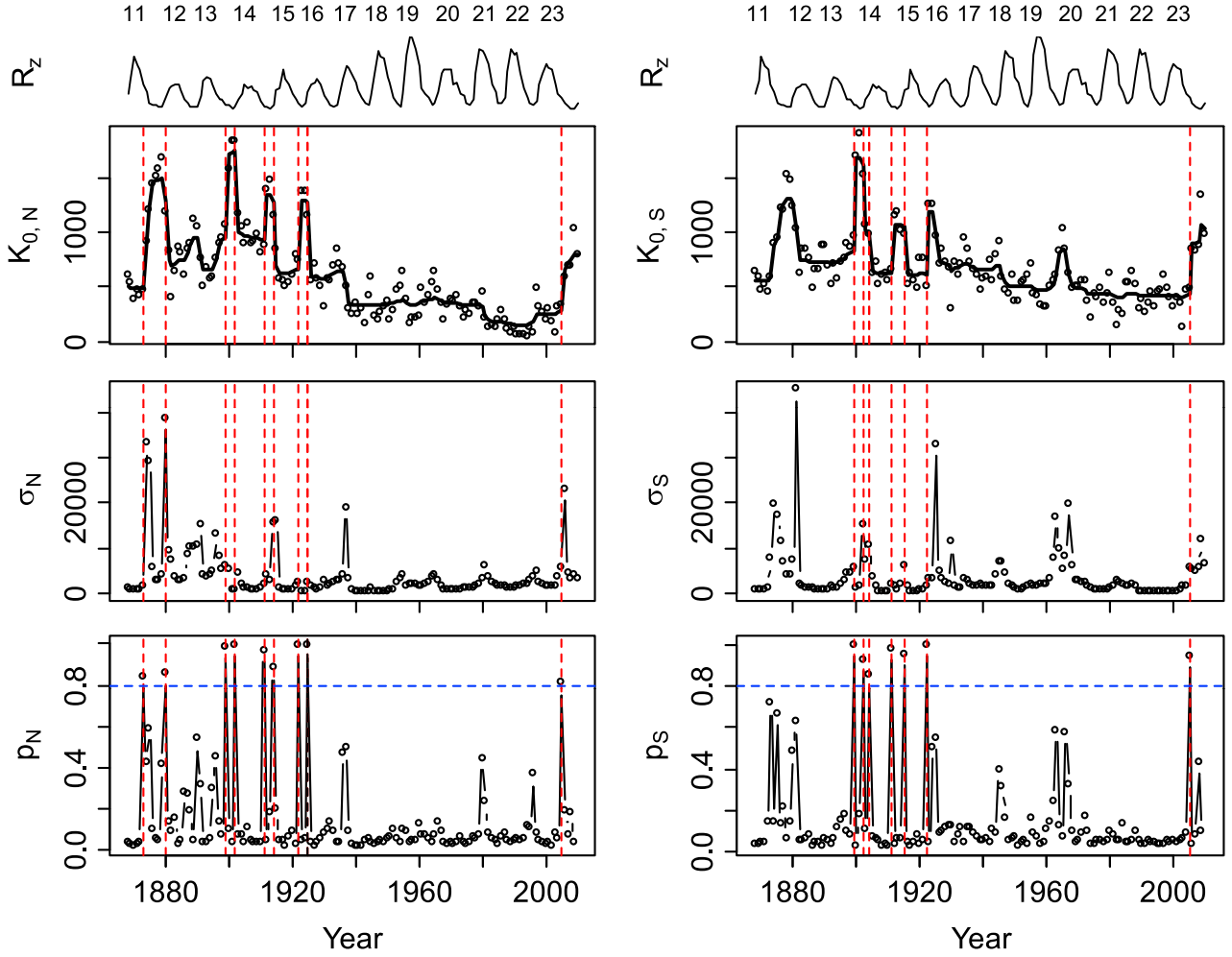

Figure 4. Bayesian analysis on the change points (sudden jumps) in (left) Northern and (right) Southern annual occurrence of $K = 0$ (K_0), with the associated Bayesian variance (σ) and probability (p) of the changes are plotted in the second and third rows of panels. The vertical red lines are those years with probability values greater than 80%, which are indicated by the blue horizontal lines in the estimated probability (bottom panels). The solar cycle number and the annual mean sunspot number for this same period are shown on the top for comparison.

Table 2. List of All the Abrupt Change Years Identified by the Bayesian Analysis With Probability >80% in Annual Occurrence of $K = 0$ ($K_{0,N}$ and $K_{0,S}$) and $K = 2$ or 3 ($K_{2|3,N}$ and $K_{2|3,S}$) for Both Northern and Southern Hemispheres[a]

Year	$K_{0,N}$	$K_{0,S}$	$K_{2|3,N}$	$K_{2|3,S}$	Ψ_{K0}
1873	0.84	*0.72	*0.61	0.90	–
1880	0.86	*0.62 (+1 yrs)	0.87	*0.70	–
1899	0.99	1.00	1.00	0.99	–
1902	1.00	0.93	0.93	0.84	–
1904	–	0.85	–	–	0.99
1911	0.97	0.98	0.97	0.96	–
1914	0.88	0.97 (+1 yrs)	0.82	0.95 (+1 yrs)	–
1922	1.00	1.00	0.97	0.95	–
1925	0.99	–	0.97	*0.71	0.82
1937	–	–	–	–	0.86
1996	–	–	–	–	1.00
2005	0.91	0.92	0.81	*0.59	–

[a]The abrupt change years in the ratio of $\Psi_{K0} = K_{0,N}/K_{0,S}$ are also listed. The abrupt change years just one year after the listed one is also shown as "+1 yr" in brackets. The probably values that start with an asterisk are below the threshold value of 0.8 but larger than 0.5; otherwise they are marked as with a dash.

(red vertical lines). The associated probability values are given in Table 2 (2nd and 3rd columns). It is clear that the posterior means of $K_{0,N}$ and $K_{0,S}$ are very similar to each other. Before 1925 or during solar cycles 11–15, there were regular, coordinated abrupt increases (decreases) of $K_{0,N}$ and $K_{0,S}$ when solar activity moved into (out of) solar minima. A similar tendency re-emerged in 2005 when solar activity reached its minimum at the end of solar cycle 23. During 1926–2005 (i.e., solar cycles 16–22) when solar activity was at its centennial-scale maximum, no abrupt changes were found in either $K_{0,N}$ or $K_{0,S}$. The abrupt changes in both $K_{0,N}$ and $K_{0,S}$ occurred primarily at the troughs of the centennial-scale variation of solar activity, implying a dominant role of the long-term variation of solar activity.

[23] Among those solar-related abrupt changes, there were two outlier years. One is 1904, which is shown as an abrupt change year in $K_{0,S}$ but not in $K_{0,N}$ and the other is 1925, which is shown as an abrupt change year in $K_{0,N}$ but not in $K_{0,S}$. In section 4.2.2, we shall demonstrate that they are most likely due to an increase of background noise level in the southern site (in the case of 1904) and site relocation from Greenwich to Abinger in 1925.

[24] Figure 5 further proves the dominant influence of solar activity on the K index. The Bayesian analysis of the

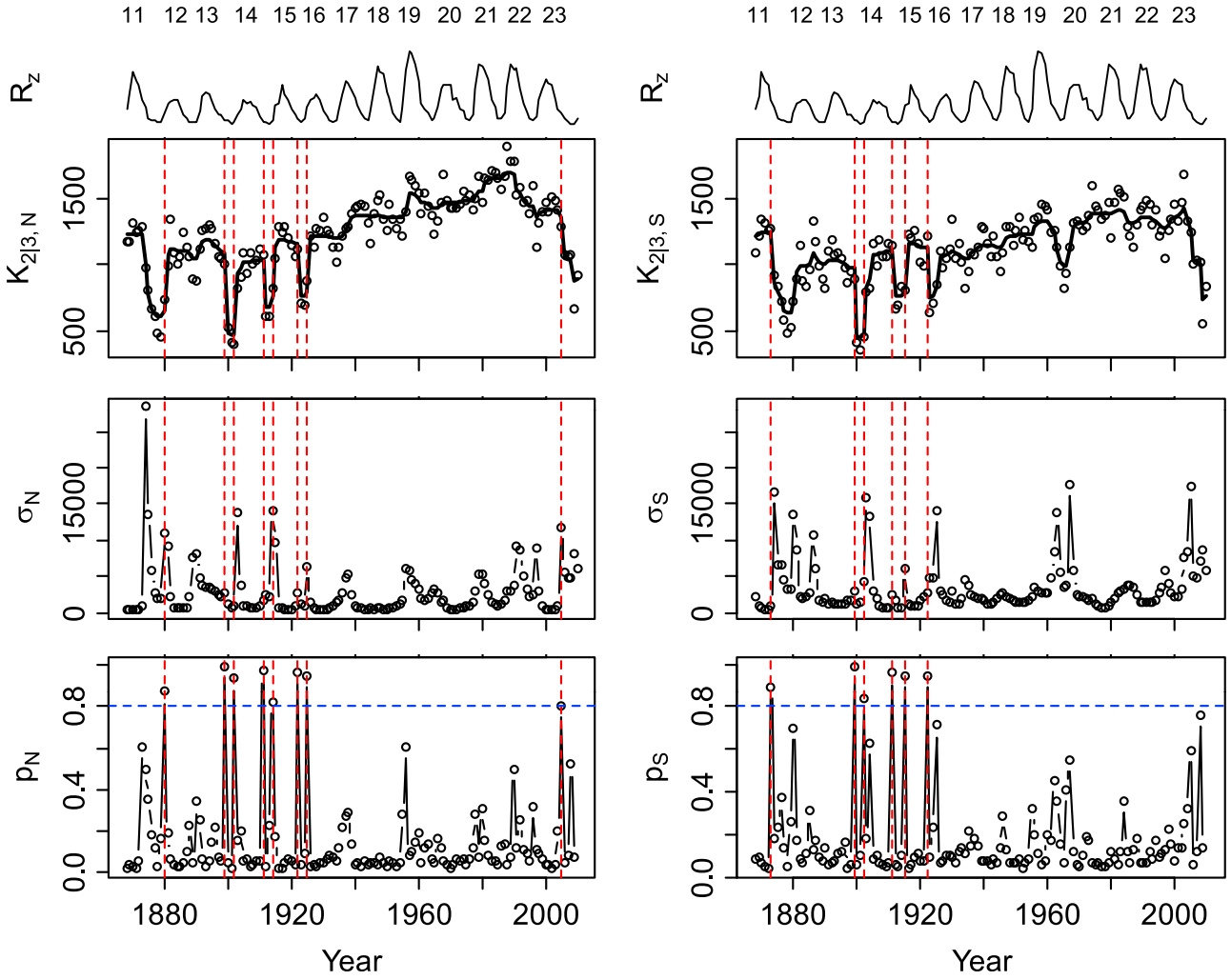

Figure 5. Same as Figure 4 but for annual occurrence of $K = 2$ or 3 ($K_{2|3}$).

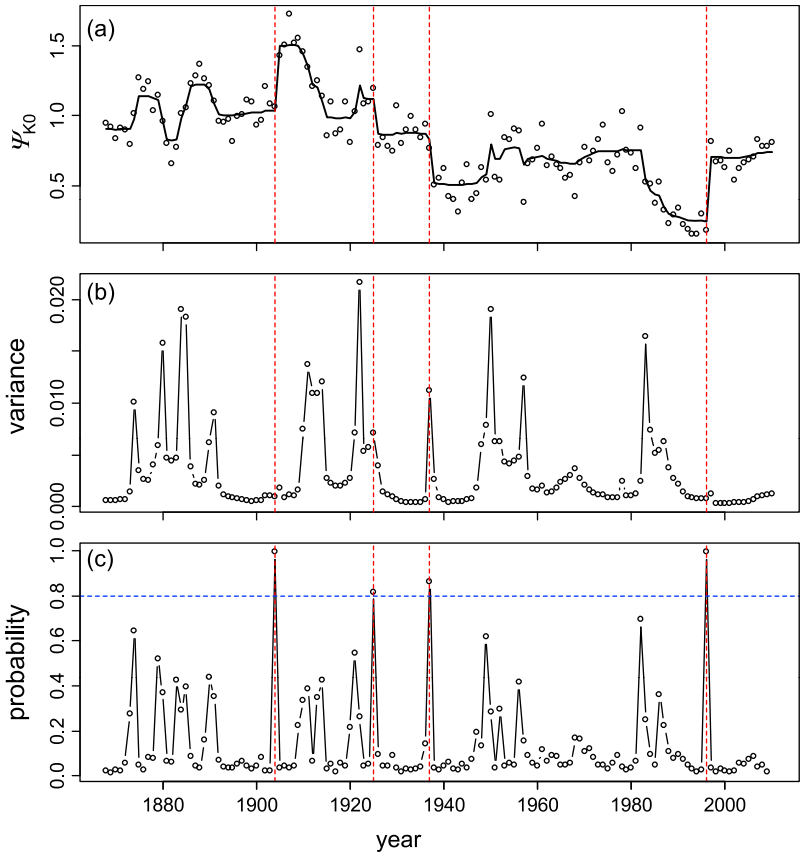

Figure 6. (a–c) Bayesian analysis on the change points (jumps) in the ratio of Northern and Southern Ψ_{K0} (north divided by south K_0). The red vertical dashed lines are the change point years (1904, 1925, 1937 and 1996) determined by probability greater than 80% (the blue dashed horizontal line in Figure 6c).

annual occurrence of $K = 2$ or 3 for the northern ($K_{2|3,N}$) and southern ($K_{2|3,S}$) sites, respectively. Similar to K_0, the posterior means of $K_{2|3,N}$ and $K_{2|3,S}$ resemble each other well. It is also clear that $K_{2|3}$ (Figure 5) and K_0 (Figure 4) vary in opposite directions for both hemispheres. That is, when $K_{2|3}$ increases, K_0 decreases and vice versa over the centennial scale. There is also remarkable agreement of the abrupt change years as detected by the Bayesian analysis (see the associated probability values in 4th and 5th columns of Table 2). The only exceptions are 1904 and 1925, which will be discussed later in section 4.2.2. These results suggest a well-coordinated response between K_0 and $K_{2|3}$ around solar minima. That is: at the minima of Gleissberg cycle, a sudden increase (decrease) of K_0 is directly associated with a sudden decrease (increase) of $K_{2|3}$ at the time when the Schwabe cycle moved into (out of) its minima.

4.2.2. Changes That Were Linked to Instrument Changes

[25] Given idealized conditions, the ratio between $K_{0,N}$ and $K_{0,S}$ ($\Psi_{K0} = K_{0,N}/K_{0,S}$), a measure of relative contribution of background noise from southern and northern sites to the total measurement of solar quiet time variation, should be equal to 1 with northern and southern observations contributing to the *aa* index equally. $\Psi_{K0} >$ (or $<$) unity indicates an increase of background noise on the quiet solar variation from the southern (or northern) site. Figure 6a shows how Ψ_{K0} (dotted) and its posterior mean (solid line) have varied with time. Before 1938, Ψ_{K0} showed a slight bias with slightly more $\Psi_{K0} > 1$ than $\Psi_{K0} < 1$, implying a larger noise level from the southern site than from the northern site. Since 1938, Ψ_{K0} were mostly smaller than 1, implying that the northern site contributed more noise than the southern site.

[26] Four most likely abrupt change years of Ψ_{K0} are detected by the Bayesian analysis. They are: 1904, 1925, 1937 and 1996 with a probability $p > 0.8$ (see Figures 6b and 6c and the last column of Table 2 for statistical details). In general, the four abrupt changes of Ψ_{K0} differ in character from those changes detected in $K_{0,N}$, $K_{0,S}$, $K_{2|3,N}$, $K_{2|3,S}$ and do not show a clear link to either solar minima or the long-term trend. The change points in 1937 and 1996 agree remarkably well with those identified by *Clilverd et al.* [2002]. Based on a different north–south asymmetry of annual occurrence of $K = 0$, defined by the normalized K_0, $(K_{0,N} - K_{0,S})/(K_{0,N} + K_{0,S})$, *Clilverd et al.* [2002] suggested that the introduction of a single LaCour magnetograph system at Abinger in 1938 might have caused a lower than expected $K_{0,N}$. They also suggested that the adaption to a new low-noise magnetometer system (known as GAUSS) at Hartland in 1997 would have resulted in improved detection of the solar-quiet variation, with consequently more accurate measurements of $K_{0,N}$ since 1998 [*Turbitt et al.*, 1999]. Here we further identify two additional abrupt changes, one in 1904 and the other in 1925; these coincide with the two

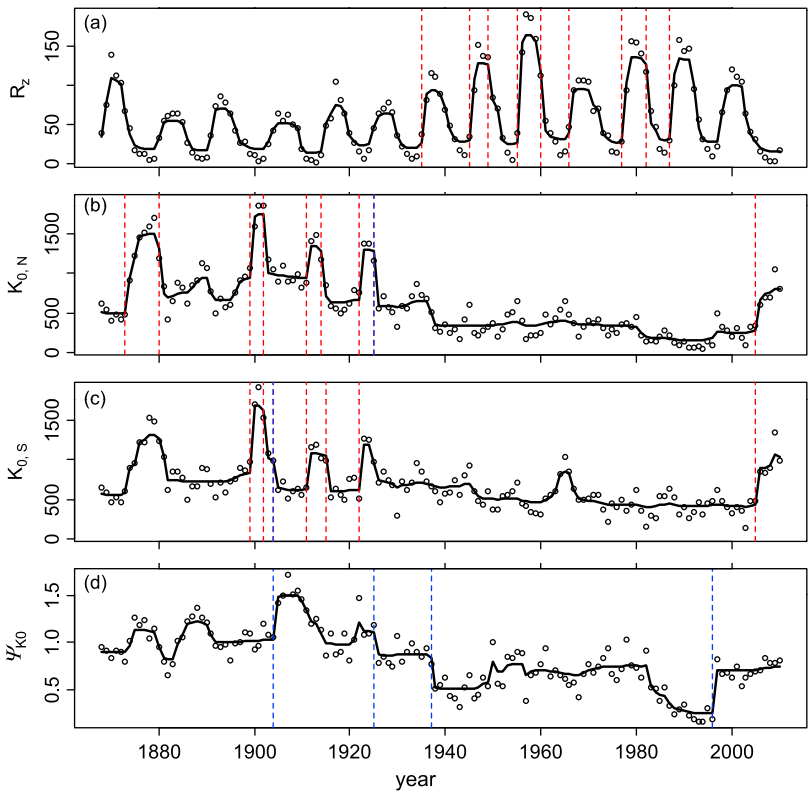

Figure 7. Sudden changes identified in (a) annual mean sunspot number (*Rz*), (b) Northern K_0 ($K_{0,N}$), (c) Southern K_0 ($K_{0,S}$), and (d) the ratio of Northern and Southern K_0 (Ψ_{K0}). The vertical dashed lines are the same as those in Figure 4 with red and blue lines indicating solar and instrumental induced changes, respectively.

outlier years identified in the Bayesian analyses of $K_{0,S}$ and $K_{0,N}$ (see Figure 4). We suggest that the abrupt change in 1925/1926 may be in part caused by site relocation of the northern site from Greenwich to Abinger. During the change, horizontal and declination variometers were installed when the Abinger observatory started its operation [*Love*, 2011b]. However, it is unlikely that the entire amplitude of the change at 1925/1926 is caused by site relocation or by instrumental change because a well-coordinated sudden increase (drop) was also visible in $K_{0,S}$ ($K_{2|3,S}$) at the time, though the corresponding changes in both $K_{0,S}$ and $K_{2|3,S}$ were only significant at smaller probability values (see the probability values marked with an asterisk in Table 2). As a maximum estimate, only up to a third of the changes in $K_{0,N}$ at the time may be attributed to site or instrumental contamination while the rest were almost certainly solar-induced changes.

[27] The increase of noise levels over the period of 1904–1914 may reflect the installation of electric grids required by electric trams around the time. The electric contamination changed the environmental conditions of Melbourne observatory dramatically and directly resulted in a new observatory being built at Toolangi, about 50 km northeast of Melbourne in 1919. Toolangi Observatory started its official operation in 1920.

[28] None of the instrumentally affected periods (i.e., 1904/1905, 1925/1926, 1937/1938, 1996/1997) were detected by the Bayesian analysis. No significant abrupt changes in any other value or subgroup values of the *K* index were detected, or in their northern and southern ratios, suggesting that instrumental contamination on the *K* index is mostly confined to the quiet time solar variation (i.e., $K = 0$).

[29] Figure 7 compares the abrupt changes identified by the Bayesian analysis for *Rz*, $K_{0,N}$, $K_{0,S}$, and $\Psi_{K0} = K_{0,N}/K_{0,S}$. In contrast to $K_{0,N}$ and $K_{0,S}$, the abrupt changes associated with *Rz* were mainly confined in the period of 1935 to 1987, during which the centennial trends of *Rz* and geomagnetic indices peaked. It is also clear that the magnitude of the changes in $K_{0,N}$ and $K_{0,S}$ around the four abrupt change periods (i.e., the blue vertical lines in Figure 7) were considerably smaller than their centennial variations. This further confirms that the abrupt changes associated with instrumental changes were not the main cause of the increase of *aa* during the 20th century. Instead, a steady increase in solar activity over the period of 1930–1980 is more likely to be the main responsible factor.

[30] The same conclusion can also be reached by assessing the overall effect of the four abrupt changes identified in K_0 on the long-term trend of *aa*. As shown in Figure 6a, the changes in 1904/1905 and 1937/1938 forced Ψ_{K0} away from unity, representing an increase of noise levels caused by instrumental changes. Those changes resulted in fewer occurrences of $K = 0$ in either the southern or northern site, and therefore may have artificially increased the *aa* index. The change in 1925/1926 reduced Ψ_{K0} from slightly above unity to slightly below; its effect on the *aa* trend is therefore either negligible or neutral. The change in 1996/1997, however, took Ψ_{K0} back closer to unity, representing a decrease

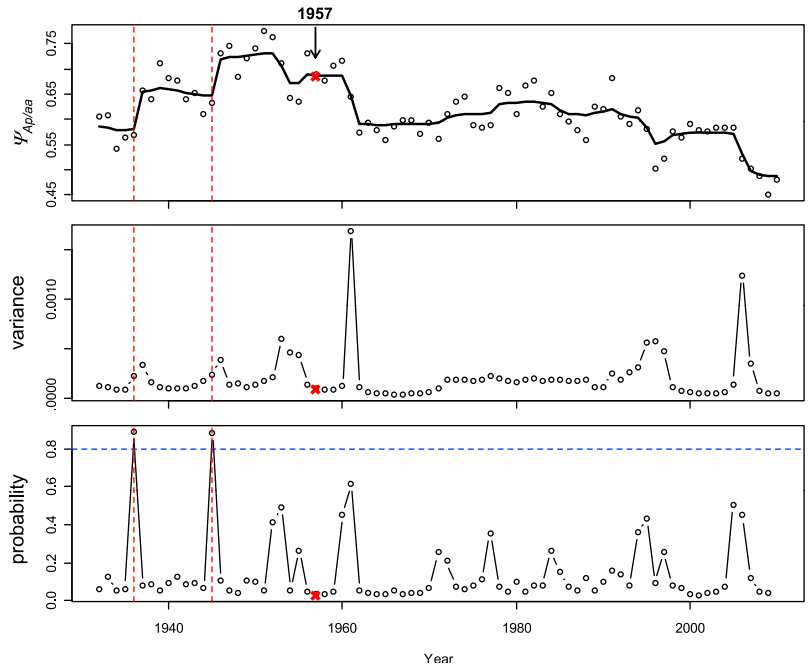

Figure 8. Bayesian analysis on the change points (jumps) in the ratio between *Ap* and *aa* ($\Psi_{Ap/aa}$). The red vertical dashed lines are the change point years (1936 and 1945) determined by probability greater than 80%. The year 1957 is highlighted for comparison.

of noise levels in the north site; this would result in higher occurrence of $K = 0$ at the northern site, causing a decrease of the *aa* index since then. In summary, we would expect an artificial increase (decrease) of the *aa* in the early (late) part of the 20th century, to cause a flatter than expected *aa* trend. Thus, if those instrumental changes have any detectable influences on the long-term variation of *aa*, they should at least not have induced the long-term trend of *aa* during 20th century. On the contrary, if a linear trend is assumed, they may have suppressed it.

4.2.3. Links to Site Relocation

[31] It is known that there were four times when the observatories were relocated, i.e., during the periods of 1919/1920, 1925/1926, 1956/1957, and 1979/1980 [*Clilverd et al.*, 2002, 2005; *Lukianova et al.*, 2009]. *Svalgaard et al.* [2004] showed a noticeable discrepancy between *aa* and IHV before 1957 and suggested that the Northern site relocation from Abinger to Hartland around 1956/1957 was the cause. *Lukianova et al.* [2009] found that stepwise increases of *aa* at the time were associated mostly with the 3-hourly *aa* values of 20–40 nT, which closely corresponds to $K = 2$ to 4 (i.e., $K_{2|4}$), and consequently suggested that the stepwise increases were most likely caused by site-specific calibration factors. As the increases aligned well with the general increase of solar activity over time, *Lukianova et al.* [2009] concluded that the calibration factors had a limited effect on the long-term trend of *aa*.

[32] Our Figure 6 shows that, during those site relocation years, Ψ_{K0} tended to have large variance as well as a larger than average probability of abrupt changes. However, the associated probability only exceeds 0.8 once – in 1925. Our Bayesian analysis also did not detect any significant jumps during the associated period in either $K_{2|3}$, $K_{2|4}$, or $K_{3|4}$. In fact, the probabilities for abrupt changes to occur at 1956/1957 for various combinations of K values, including K_1, $K_{>3}$, $K_{>4}$, and $K_{>5}$, etc, and their northern-southern ratios, are mostly below 0.5. The only exception is $\Psi_{K0|1}$, where $K_{0|1,N}$ was found to be significantly smaller than $K_{0|1,S}$ since 1957 ($p = 0.82$), implying more background noise from the northern site than from the southern site. However, no significant change of $K_{0|1,N}$ was identified at the time and the associated magnitude of the difference in $K_{0|1}$ in the north and south sites is about one order of magnitude smaller than its centennial variation (not shown). The probability for larger K values cannot be estimated accurately due to smaller sample sizes; those large K values also contribute considerably less to annual mean *aa* compared with $K = 0$–4 [*Love*, 2011b]. Thus, apart for 1925/1926, none of the other site relocation years (i.e., 1919/1920, 1956/1957, and 1979/1980) were identified by the Bayesian analysis to give a significant sudden rise in any subgroup of the K index.

[33] To further examine whether or not site relocation had any detectable effect on long-term *aa* trend, we applied the Bayesian analysis to the ratio of annual mean *Ap* and *aa* ($\Psi_{Ap/aa}$) for their common period of 1932–2010. Figure 8 shows that $\Psi_{Ap/aa}$ was generally larger and with larger variation before ~1960 than afterward, implying a greater dissimilarity between *Ap* and *aa* trends before ~1960. Furthermore, the Bayesian analysis identifies two abrupt change years, i.e., 1936 and 1946, in which $\Psi_{Ap/aa}$ increased suddenly afterward. Another likely change period is 1960–1962, during which $\Psi_{Ap/aa}$ decreased. Nevertheless, none of those years coincide with the site-relocation years. The probability of an abrupt change in 1956/1957 is close to zero, and it is associated with a rather flat posterior mean and small variance at the time. Small probability of sudden change is also

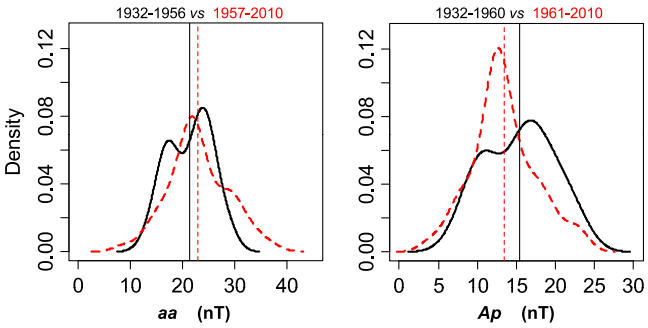

Figure 9. (left) Probability density distributions (PDFs) of the annual mean *aa* index for the sub-periods of 1932–1956 (black) and 1957–2010 (red). (right) PDFs of annual mean *Ap* index for the sub-periods of 1932–1960 (black) and 1961–2010 (red). The vertical lines indicate the mean values of the PDFs.

obtained for 1979/1980 during which the southern site relocated from Toolangi to Canberra.

[34] Based on conventional statistical methods, Figure 9 compares the probability density functions (PDFs) of annual mean *aa* and *Ap* indices where *aa* is artificially separated into two sub-periods of 1932–1956 and 1957–2010, while *Ap* is broken into two sub-periods of 1932–1960 and 1961–2010. When *aa* is separated at 1956/1957, both the PDF and mean differences between the early and late sub-periods are not statistically significant, with the *p-values* equal to 0.26 and 0.71 respectively. The *p-value* of the PDF difference is estimated based on a Kolmogorov-Smirnoff test [*Press et al.*, 1992] while the *p-value* of the mean difference is calculated using Wilcoxon-Mann-Whitney rank sum test [*Iman*, 1994]. Conversely, a significant difference (with a *p-value* = 0.016) between the two PDFs for the early and late sub-periods can be established for *Ap* before and after 1960. Moreover, the mean values of these two sub-periods are also significantly different from each other (with a *p-value* = 0.08). It suggests that the planetary *Ap* index had a significant change of structure around 1960/1961 and the change is marked by the different shaped PDFs and ~2 nT reduction of mean value since 1960/1961. Thus, the long-term trend of *Ap* was not stationary during 20th century. The sudden drop of the ratio $\Psi_{Ap/aa}$ in Figure 8 is most likely due to this non-stationary behavior of *Ap*.

[35] We therefore conclude that there is little statistical evidence to suggest that instrumental change or site relocation have made significant changes of long-term variation of *aa*. In particular, site-relocation from Abinger to Hardland around 1956/1957 cannot be the primary cause for the observed deviation among geomagnetic indices.

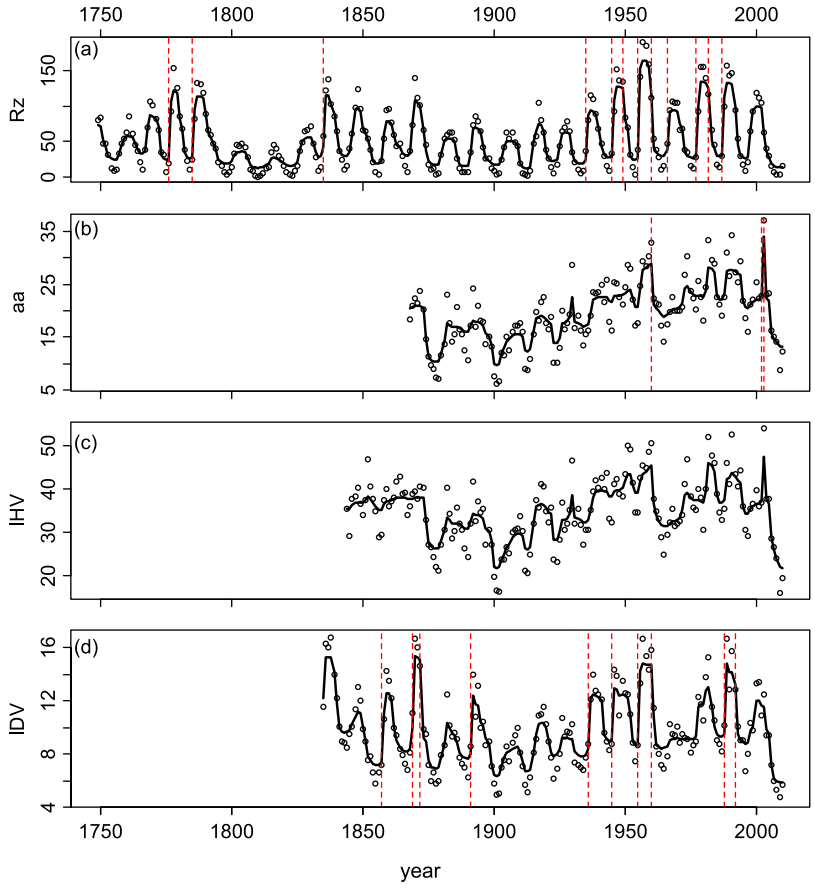

Figure 10. Sudden changes in annual (a) *Rz*, (b) *aa*, (c) IHV, and (d) IDV identified as probability of change great than 0.8. Note that there is no sudden jump found in IHV with probability higher than 0.8. See Table 3 for further details.

Table 3. List of All the Sudden Change Years With Probability >80% in Either Annual Mean *Rz*, aa, IHV, or IDV[a]

Year	Rz	aa	IHV	IDV
1776 (a)	0.98	No data	No data	No data
1785 (a)	0.89	No data	No data	No data
1835 (a)	0.93	No data	No data	No data
1857 (a)	*0.73	No data	–	0.80
1869 (a)	*0.51	–	–	0.92
1872 (d)	*0.61	*0.65 (+1 yr)	*0.54 (+1 yr)	0.97
1891 (a)	*0.67	–	–	0.94
1919 (d)	*0.64	–	–	–
1935 (a)	0.91	–	–	0.88 (+1 yr)
1945 (a)	0.97	–	–	0.97
1949 (d)	0.81	–	–	–
1955 (a)	1.00	–	–	0.95
1960 (d)	0.89	0.84	*0.72	0.81
1966 (a)	0.87	–	–	–
1977 (a)	0.94	–	–	*0.76
1982 (d)	0.92	–	–	–
1987 (a)	0.97	*0.66 (+1 yr)	–	0.97 (+1 yr)
1992 (d)	*0.74	–	–	0.80
2002 (d)	*0.66	0.88	*0.71	*0.55 (+1 yr)

[a]The list shows that all the years are either in the ascending (a) or descending (d) phases of the 11-year solar cycle. If the probability >50%, the actual value of the probability is given with an asterisk in front. Otherwise it is marked with a dash. For simple approximation, we also allow *Rz* to lead geomagnetic indices by one year with any sudden jumps occurring just one year after *Rz* shown as "+1 yr" in brackets.

Nevertheless, the Bayesian analyses presented in this section cannot deny the existence of errors caused by instrumental change or site-relocation. They are only too small to be detected statistically as major abrupt changes.

4.3. Abrupt Changes in Solar and Geomagnetic Activity

[36] Figure 10 shows the abrupt change points of the annual mean *Rz*, *aa*, IHV and IDV, where the Bayesian analyses were performed based on the full record of each index. The associated years and the probability of a sudden change for the identified years are given in Table 3. These suggest that a sudden change of *Rz* was more likely to occur at the peaks of its centennial trend and in the ascending phase of the 11-yr solar cycle. Similar behavior is found in IDV. In contrast, only two abrupt changes were detected in *aa* and no abrupt change was found in IHV. This confirms a closer relationship exists between IDV and *Rz* than between *aa* (or IHV) and *Rz*. As the main source of the equatorial component of the Sun's large-scale magnetic field is large active regions which can be associated with *Rz*, it is reasonable to expect sudden changes in the IDV index to be corresponding well with sudden changes in *Rz*. The response of the annual mean solar wind to sudden changes in sunspot number is presumably a complex interplay between the occurrence of high speed solar winds events caused by CIRs and CMEs during those periods. The differences in abrupt changes in *aa*, IHV and IDV are expected as different geomagnetic indices respond differently to different combinations of the IMF field strength *B* and the solar wind speed *V* [*Lockwood et al.*, 2009; *Lockwood and Owens*, 2011]. Nevertheless, none of the instrumental or site relocation years were found to make a significant change to the annual mean *aa*.

[37] To further check the robustness of the analysis, we also applied the Bayesian analysis to annual mean *Ap* index. A significant change in 1960 was also found in *Ap* with a probability of 0.84. The change around 2002–2003 remained the second largest but became less pronounced with a probability of 0.71.

5. Discussion

[38] Previous studies tended to use running averages to remove the 11-yr solar cycle variation and to reveal the underlying long-term drift [*Lockwood et al.*, 1999; *Svalgaard et al.*, 2004; *Svalgaard and Cliver*, 2005; *Le Mouël et al.*, 2009]. Here we use a more advanced statistical method that allows us to separate a slow varying long-term trend from cyclic and irregular variations. We have found that the amplitude ratio between the centennial-scale variation and 11-year cycle of *Rz* and IDV are comparable (39% versus 48%), while the equivalent ratios for *aa* and IHV (81% and 80% respectively) are also comparable, despite being proportionally bigger and those of *Rz* and IDV. In addition, we have shown that the centennial-scale trends in three long-term geomagnetic indices are nearly identical to each other and varied in phase with the *Rz*. Thus, our results support the conclusion of *Demetrescu and Dobrica* [2008] that both electromagnetic radiation (reflected by *Rz*) and corpuscular flux (reflected by *aa*) in the near-Earth heliosphere are subject to the same centennial variation.

[39] *Svalgaard et al.* [2004] show a discrepancy between *aa* and IHV before 1957 and the discrepancy was estimated as large as 5–10 nT in the first two decades of the 20th century. Trend difference between *aa* and *Ap* was also reported by *Lockwood et al.* [2009]. *Love* [2011b] has noted that the *K* indices from south and north observatories tend to have different distributions of occurrence which may lead to a bias in the resulting occurrence distribution and long-term change of the *aa* index. Here we confirm that such discrepancies and bias do exist. But they are unlikely to be caused by instrumental change or site relocation of the official *aa* sites. In particular, there is also little statistical evidence to support the notion that the site relocation from Abinger to Hartland during 1956/1957 has caused a substantial change of *aa* or its long-term trend. Other factors must be involved in order to explain the discrepancy among *aa*, *Ap* and IHV [*Svalgaard et al.*, 2004]. This conclusion is consistent with previous studies [*Clilverd et al.*, 1998, 2002, 2005; *Lukianova et al.*, 2009].

[40] Our results are also in good agreement with *Love* [2011a], who suggested that the detailed secular evolution of geomagnetic activity cannot be well characterized by either a linear or monotonic trend. For instance, the well-known tendency for magnetic storms to occur during the declining phase of the Schwabe cycle is only clear for cycles 14–23; it is not clear for earlier cycles (e.g., 11–13). Significant abrupt changes of geomagnetic indices also negate the existence of simple linear trends over the centennial-scale. In fact, our analysis has demonstrated that the long-term variation of geomagnetic activity is both nonlinear and non-stationary.

[41] *Svalgaard et al.* [2004] show that the IHV index is approximately proportional to BV^2 and consequently suggest

that the IHV index reacts to heliospheric conditions in a similar way to the *aa* index. *Svalgaard and Cliver* [2005] found that the IDV index is empirically correlated with the near-Earth IMF strength B and it is also correlated to the square root of the sunspot number *Rz*. These findings suggest that the near-Earth IMF variation at decadal to centennial scales depends mainly on a combination of B and V. Other studies suggested that the geomagnetic dependence on B and V is more complicated and can be influenced by Earth's magnetic dipole moment [*Stamper et al.*, 1999; *Lockwood and Owens*, 2011]. Given the fact that geomagnetic activity is nonlinear and non-stationary, caution is needed when extend empirical regressions back or forward in time.

6. Conclusions

[42] With all the three long-term geomagnetic indices (i.e., *aa*, IHV and IDV), our STL decomposition shows that they all share a similar centennial-scale variation that resembles the long-term trend of sunspot number *Rz*. The centennial-scale variation is shown to have an $80 \sim 100$ year periodicity which is in phase with the well-known Gleissberg cycle.

[43] The Bayesian change point detection suggests that the majority of the abrupt changes in annual *aa* or *K* indices were controlled by solar activity. Although the Bayesian analysis cannot rule out the existence of changes associated with instrumental change or site-relocation, those changes are too small to be detected statistically. Therefore, they are unlikely to have altered the long-term trend of *aa* significantly.

[44] The conclusion is made on the basis of our analysis that a simple stepwise correction of *aa* around the time when instrumental change or site-relocation took place may not result in a proper correction of *aa*. A correction of this kind may introduce a large and uncalculated uncertainty, making it harder to detect and to understand the true cause of the discrepancy among geomagnetic indices.

Appendix A: STL Decomposition

[45] The decomposition algorithm used here is the *S*easonal-*T*rend decomposition based on *L*OESS (STL) of *Cleveland et al.* [1990]. LOESS fits a smoothed time series $\tilde{X}(j)$ to an input series $X(j) = X(t_j)$, where t_j is a sequence of discrete sampling times. The smoothed value at each point j is given by the value at time t_j of a polynomial fitted to the sampled values of X over a window $(j - q, j + q)$ with decreasing weight assigned to points in this window as their distance from point j increases.

[46] In outline, the STL decomposition generates three additive components from the time series $X(j)$: a long-term trend X_T, a cyclic component X_C with a pre-defined period n_P, and a residual component X_R: $X(j) = X_T(j) + X_C(j) + X_R(j)$. The STL decomposition consists of outer and inner loops with a sequence of smoothing operator LOESS for the purposes of detrending, deseasonalizing and reducing the influence of transient, aberrant behavior on both the trend and cyclic components. Implementing the algorithm involves six major steps.

[47] 1. The slow varying trend component $X_T(j)$ is found by LOESS smoothing over a span window $(j - n_t, j + n_t)$.

[48] 2. The residual series $X(j) - X_T(j)$ is grouped into n_p cyclic-subseries, where n_p is number of sample points in the cyclic period (i.e., 11 years in our case). Each cyclic-subseries consists of $\{X(m) - X_T(m), X(m + n_p) - X_T(m + n_p), X(m + 2n_p) - X_T(m + 2n_p), \ldots\}$, where m varying from 1 to n_p.

[49] 3. The cyclic-subseries are individually smoothed using LOESS with one degree of locally fitted polynomial for the subseries low-pass filter with a span window $(m - n_s, m + n_s)$, and the low-pass filtered subseries are then recombined into a complete series using LOESS with a span window size of $2n_l + 1$. The result becomes a first estimate of the cyclic component $X_C(j)$.

[50] 4. A first estimate of the residual component is calculated as $X_R(j) = X(j) - X_T(j) - X_C(j)$.

[51] 5. A "robustness weight" is assigned to each point $X(j)$ based on the estimated $X_R(j)$. The weight decreases as $|X_I(j)|$ increases.

[52] 6. Steps 1 to 5 are repeated until convergence, with weights in all LOESS smoothing operations including the robustness weights for every point in the series. The convergence of STL from successive iterations k to $k + 1$ of either a trend or seasonal component was judged by the following criterion:

$$\frac{\max_j \left| V^k(j) - V^{k+1}(j) \right|}{\max_j V^k(j) - \min_j V^k(j)} < 0.01 \tag{A1}$$

where $V = X_T$ or X_C for the cases of the trend or cyclic component, respectively.

[53] The STL procedure has been implemented as an internal function stl in R package named "stats" by R Development Core Team (http://CRAN.R-project.org), which provides an easy access to this method, including further detailed introduction, explanation and description about this method. The implementation involves a few parameters that determine the degree of the smoothing in both trend and cyclic components. Namely, n_p is periodicity of the cyclic component; n_s and n_t define the span window sizes of the cyclic and trend components, and n_l is the span-window parameter for the subseries low-pass filter. The user also requires defining the degrees of locally fitted polynomial in seasonal, trend extraction and the subseries low-pass filter, respectively.

[54] In this study, where annual geomagnetic indices and sunspot number are known to have a distinct quasi-11-year cyclic variation, $n_p = 11$, $n_l = n_p$, $n_t = 51$, $n_s = 5$ are used. The degrees of locally fitted polynomial in seasonal, trend extraction and the subseries low-pass filter are taken as 0, 1 and 1, respectively Those values were chosen according to the guidelines given in *Cleveland et al.* [1990]. We have found that the application of STL to all four time series (i.e., *Rz*, *aa*, IHV and IDV) is not sensitive to the values of n_l, n_t, and n_s as long as $n_t \gg n_s$. In addition, our sensitivity test shows that quantitatively similar results can be obtained if n_p is set to 10 or 12 as STL only assumes quasiperiodicity of the cyclic component.

Appendix B: Bayesian Change Point Detection

[55] *Barry and Hartigan* [1993] proposed a Bayesian model for multiple change point problems. This estimates both the posterior means and the posterior probability of a change for each position sequence. Namely, when there is an unknown partition ρ in a given time series $\boldsymbol{X}$, of a set into contiguous segments, which is defined as a period of time between two consecutive change points within which the means are equal. The model assumes that observations obey normal distribution $N(\mu_i, \sigma^2)$, and the probability of a change point at a position i is p that is independently at each i. The prior distribution of μ_{ij} (the mean of the segment beginning at position $i + 1$ and ending at position j) is chosen as $N(\mu_0, \sigma_0^2/(j - i))$. Note that the variance of the prior changes with the length if the segment; specifically, larger deviations from μ_0 are expected in shorter segment. That is, the model does not expect to detect a small change in mean if it persists for a short time. The priors of μ_0, p, σ^2 and the ratio of signal to error variance $w = \sigma^2/(\sigma^2 + \sigma_0^2)$ are defined as:

$$
\begin{aligned}
&f(\mu_0) = 1, -\infty \le \mu_0 \le \infty \\
&f(\sigma^2) = 1, -\infty \le \sigma^2 \le \infty \\
&f(p) = 1/p_0, \quad 0 \le p \le p_0 \\
&f(w) = 1/w_0, \quad 0 \le w \le w_0 \\
&f(\rho) = \frac{1}{p_0}\left[\int_0^{p_0} p^{b-1}(1-p)^{n-b}dp\right]
\end{aligned}
$$

where $f(x)$ stands for prior probability of x, p_0 and w_0 are preselected numbers in [0, 1] and b is the number of segment in the partition.

[56] A Markov chain Monte Carlo (MCMC) implementation of *Barry and Hartigan*'s [1993] model was proposed by *Erdman and Emerson* [2007]. For a time series $\boldsymbol{X}$, the algorithm uses a segment partition $\rho = (U_1, U_2, \ldots, U_n)$, where n is the number of observations in $\boldsymbol{X}$ and $U_i = 1$ indicates a change point at position $i + 1$. It starts with an initialization of $U_i = 0$ for all $i < n$ and $U_n \equiv 1$. In each step of the MCMC and at each position of i, a value of U_i is drawn from the conditional distribution of U_i defined by the data and the current partition. If $U_i = 0$, conditional on U_j, for $i \ne j$, the transition probability, p, for the conditional probability of a change point at the position $i + 1$, is obtained from the ratio:

$$
\begin{aligned}
\frac{p_i}{1-p_i} &= \frac{P(U_i = 1|\mathrm{X}, U_j, j \ne i)}{P(U_i = 0|\mathrm{X}, U_j, j \ne i)} \\
&= \frac{\left[\int_0^{\gamma} p^b(1-p)^{n-b-1}dp\right]\left[\int_0^{\lambda} \frac{w^{b/2}}{(W_1 + B_1 w)^{(n-1)/2}}\right]}{\left[\int_0^{\gamma} p^{b-1}(1-p)^{n-b}dp\right]\left[\int_0^{\lambda} \frac{w^{(b-1)/2}}{(W_0 + B_0 w)^{(n-1)/2}}\right]}
\end{aligned}
\tag{B1}
$$

where W_0, B_0, W_1, and B_1 are the within and between segment sums of squares obtained when $U_i = 0$ and $U_i = 1$ respectively. γ and λ are tuning parameters that take values in [0, 1]. They are chosen so that this method is effective in situations where there are not too many changes (i.e., γ is small), and where the changes that do occur are of reasonable size (i.e., λ is small). The various sums of squares (W_0, B_0, W_1, and B_1) in consecutive steps of the algorithm are updated after each iteration. The R implementation of the Bayesian approach is available on CRAN as the "bcp" package [*Erdman and Emerson*, 2007] (http://CRAN.R-project.org). We use the default values of $p_0 = 0.2$ and $w_0 = 0.2$ which has been found to work well with a wide range of time series [*Erdman and Emerson*, 2007]. The number of iterations used to estimation the posterior means is also set as the default value (500).

[57] **Acknowledgments.** H.L., M.J.J., and M.A.C. were supported by the UK Natural Environment Research Council (NERC). Y.L. was supported by the CSIRO Climate Adaptation Flagship and the Indian Ocean Climate Initiative Project. We are grateful to Ellen Clarke at British Geographic Survey (http://www.geomag.bgs.ac.uk) for the access of the 3-hourly *K*-indices, annual *aa*, and *Ap* indices. We also thank Leif Svalgaard for providing annual mean IHV and IDV indices and for useful discussions. Finally, we thank two anonymous reviewers for their constructive comments.

[58] Robert Lysak thanks the reviewers for their assistance in evaluating this paper.

References

Barry, D., and J. A. Hartigan (1993), A Bayesian analysis for change point problems, *J. Am. Stat. Assoc.*, *88*, 309–319, doi:10.2307/2290726.

Bartels, J. (1932), Terrestrial-magnetic activity and its relations to solar phenomena, *Terr. Magn. Atmos. Electr.*, *37*(1), 1–52, doi:10.1029/TE037i001p00001.

Cleveland, W. S., and S. J. Devlin (1988), Locally weighted regression: An approach to regression analysis by local fitting, *J. Am. Stat. Assoc.*, *83*(403), 596–610, doi:10.2307/2289282.

Cleveland, R. B., W. S. Cleveland, J. E. McRae, and I. Terpenning (1990), STL: A seasonal-trend decomposition procedure based on LOESS, *J. Off. Stat.*, *6*, 3–73.

Clilverd, M. A., T. D. G. Clark, E. Clarke, and H. Rishbeth (1998), Increased magnetic storm activity from 1868 to 1995, *J. Atmos. Sol. Terr. Phys.*, *60*, 1047–1056, doi:10.1016/S1364-6826(98)00049-2.

Clilverd, M. A., T. D. G. Clark, E. Clarke, H. Rishbeth, and T. Ulich (2002), The causes of long-term change in the *aa* index, *J. Geophys. Res.*, *107*(A12), 1441, doi:10.1029/2001JA000501.

Clilverd, M. A., E. Clarke, T. Ulich, J. Linthe, and H. Rishbeth (2005), Reconstructing the long-term *aa* index, *J. Geophys. Res.*, *110*, A07205, doi:10.1029/2004JA010762.

Cliver, E. W., V. Boriakoff, and J. Feynmann (1998), Solar variability and climate change: Geomagnetic aa index and global surface temperature, *Geophys. Res. Lett.*, *25*, 1035–1038, doi:10.1029/98GL00499.

Demetrescu, C., and V. Dobrica (2008), Signature of Hale and Gleissberg solar cycles in the geomagnetic activity, *J. Geophys. Res.*, *113*, A02103, doi:10.1029/2007JA012570.

Erdman, C., and J. W. Emerson (2007), bcp: An R package for performing a Bayesian analysis of change point problems, *J. Stat. Softw.*, *23*(4), 1–13.

Erdman, C., and J. W. Emerson (2008), A fast Bayesian change point analysis for the segmentation of microarray data, *Bioinformatics*, *24*, 2143–2148, doi:10.1093/bioinformatics/btn404.

Feynman, J., and N. U. Crooker (1978), The solar wind at the turn of the centrury, *Nature*, *275*, 626–627, doi:10.1038/275626a0.

Gonzalez, W. D., B. T. Tsurutani, and A. L. Clua de Gonzalez (1999), Interplanetary origin of geomagnetic storms, *Space Sci. Rev.*, *88*, 529–562, doi:10.1023/A:1005160129098.

Hegarty, A., and D. Barry (2008), Bayesian disease mapping using product partition models, *Stat. Med.*, *27*, 3868–3893, doi:10.1002/sim.3253.

Iman, R. L. (1994), *A Data-Based Approach to Statistics*, 348 pp., Duxbury, Pacific Grove, Calif.

Isotta, F., O. Martius, M. Sprenger, and C. Schwierz (2008), Long-term trends of synoptic-scale breaking Rossby waves in the Northern Hemisphere between 1958 and 2001, *Int. J. Climatol.*, *28*, 1551–1562, doi:10.1002/joc.1647.

Johnson, T. D., R. M. Elashoff, and S. J. Harkema (2003), A Bayesian change-point analysis of electromyographic data: Detecting muscle activation patterns and associated applications, *Biostatistics*, *4*, 143–164, doi:10.1093/biostatistics/4.1.143.

Koop, G., and S. Potter (1997), Nonlinearity, structural breaks or outliers in economic time series?, in *Nonlinearity and Econometrics*, edited by W. Barnett et al., pp. 61–78, Cambridge Univ. Press, Cambridge, U. K.

Le Mouël, J. L., E. Blanter, M. Shnirman, and V. Courtillot (2009), Evidence for solar forcing in variability of temperatures and pressures in

Europe, *J. Atmos. Sol. Terr. Phys.*, *71*(12), 1309–1321, doi:10.1016/j.jastp.2009.05.006.

Li, Y., E. P. Campbell, D. Haswell, R. J. Sneeuwjagt, and W. N. Venables (2003), Statistical forecasting of soil dryness index in the southwest of Western Australia, *For. Ecol. Manage.*, *183*, 147–157, doi:10.1016/S0378-1127(03)00103-8.

Lockwood, M., and M. J. Owens (2011), Centennial changes in the heliospheric magnetic field and open solar flux: The consensus view from geomagnetic data and cosmogenic isotopes and its implications, *J. Geophys. Res.*, *116*, A04109, doi:10.1029/2010JA016220.

Lockwood, M., R. Stamper, and M. N. Wild (1999), A doubling of the Sun's coronal magnetic field during the past 100 years, *Nature*, *399*, 437–439, doi:10.1038/20867.

Lockwood, M., A. P. Rouillard, and I. D. Finch (2009), The rise and fall of open solar flux during the current grand solar maximum, *Astrophys. J.*, *700*, 937–944, doi:10.1088/0004-637X/700/2/937.

Love, J. J. (2011a), Secular trends in storm-level geomagnetic activity, *Ann. Geophys.*, *29*, 251–262, doi:10.5194/angeo-29-251-2011.

Love, J. J. (2011b), Long-term biases in geomagnetic *K* and *aa* indices, *Ann. Geophys.*, *29*, 1365–1375, doi:10.5194/angeo-29-1365-2011.

Lu, H., M. R. Raupach, T. R. McVicar, and D. J. Barrett (2003), Decomposition of vegetation cover into woody and herbaceous components using AVHRR NDVI time series, *Remote Sens. Environ.*, *86*, 1–18, doi:10.1016/S0034-4257(03)00054-3.

Lukianova, R., G. Alekseev, and K. Mursula (2009), Effects of station relocation in the *aa* index, *J. Geophys. Res.*, *114*, A02105, doi:10.1029/2008JA013824.

Mayaud, P.-N. (1972), The *aa* indices: A 100-year series characterizing the magnetic activity, *J. Geophys. Res.*, *77*, 6870–6874, doi:10.1029/JA077i034p06870.

Mursula, K., and D. Martini (2007), A new verifiable measure of centennial geomagnetic activity: Modifying the K index method for hourly data, *Geophys. Res. Lett.*, *34*, L22107, doi:10.1029/2007GL031123.

Newell, P. T., T. Sotirelis, K. Liou, C.-I. Meng, and F. J. Rich (2007), A nearly universal solar wind-magnetosphere coupling function inferred from 10 magnetospheric state variables, *J. Geophys. Res.*, *112*, A01206, doi:10.1029/2006JA012015.

Press, W. H., B. P. Flannery, S. A. Teukolsky, and W. T. Vetterling (1992), *Numerical Recipes in C: The Art of Scientific Computing*, 2nd ed., 848 pp., Cambridge Univ. Press, New York.

Stamper, R., M. Lockwood, M. N. Wild, and T. D. G. Clark (1999), Solar causes of the long term increase in geomagnetic activity, *J. Geophys. Res.*, *104*, 28,325–28,342, doi:10.1029/1999JA900311.

Svalgaard, L., and E. W. Cliver (2005), The *IDV* index: Its derivation and use in inferring long-term variations of the interplanetary magnetic field strength, *J. Geophys. Res.*, *110*, A12103, doi:10.1029/2005JA011203.

Svalgaard, L., and E. W. Cliver (2010), Heliospheric magnetic field 1835–2009, *J. Geophys. Res.*, *115*, A09111, doi:10.1029/2009JA015069.

Svalgaard, L., E. W. Cliver, and P. Le Sager (2003), Determination of interplanetary magnetic field strength, solar wind speed and EUV irradiance, 1890–2003, paper presented at Solar Variability as an Input to the Earth's Environment. International Solar Cycle Studies (ISCS) Symposium, Sci. Comm. on Solar-Terr. Phys., Tatranská Lomnica, Slovakia, 23–28 June.

Svalgaard, L., E. W. Cliver, and P. Le Sager (2004), IHV: A new long-term geomagnetic index, *Adv. Space Res.*, *34*, 436–439, doi:10.1016/j.asr.2003.01.029.

Turbitt, C. W., C. J. Riddick, and S. Flower (1999), GAUSS Geomagnetic Automatic Unmanned Sampling System, Hardware and service manual, *Tech. Rep. WM/99/17*, Br. Geol. Surv., Cambridge, U. K.